CASE STUDIES ON THE TAILORING OF FGM ELASTIC HOLLOW SPHERES, CIRCULAR CYLINDERS AND DISKS USING PRACTICAL DESIGN CONDITIONS

ŞTEFAN SOROHAN , DAN MIHAI CONSTANTINESCU*, DRAGOŞ ALEXANDRU APOSTOL

Abstract. In current literature it was demonstrated that using a radial functionally graded material (FGM) may improve designing of thick spheres, cylinders and disks if the circumferential stress component or the maximum shear stress should be constant along the body radius r. These bodies are designed in one of these stress conditions and considering additional assumptions are called equal stress structures. An isotropic FGM may be characterized in linear static analyses by two elastic constants: Young's modulus $E(r)$ and Poisson's ratio $\nu(r)$. Usually, FGMs are made from two base materials, and the effective properties are obtained through homogenization. In this paper, a general stress condition, including equal strength structure, is imposed and the inverse problem is solved iteratively using a finite element model and an algorithm of stress condition uniformization. Six case studies are presented in detail, pointing out the robustness of the algorithm and the advantages of designing according to a uniform stress condition.

Key words: Functionally graded thick-walled shells, Finite element analysis, Iterative technique, Equal stress structure, Equal strength structure.

1. INTRODUCTION

Stresses distribution in an isotropic and homogeneous axisymmetrical body show their maximum values in a limited region. If the topology is fixed, as in the case of pressurized axisymmetrical bodies, the variation of the stresses can be modified by changing the material properties according to a constitutive law as to obtain the same maximum equivalent stress in a larger domain, preferably in the whole structure. Such a problem may be defined as an optimization case.

An inhomogeneous and isotropic material is locally defined through Young's modulus E and Poisson's ratio v. It may have important variations of the Young's

Department of Strength of Materials, National University of Science and Technology Politehnica of Bucharest, Splaiul Independenţei 313, Bucharest 060042, Romania
*corresponding author

Ro. J. Techn. Sci. − Appl. Mechanics, Vol. 70, N° 1−3, P. 23−52, Bucharest, 2025

DOI:10.59277/RJTS-AM.2025.1-3.02

modulus, usually within one order of magnitude, and some variations in Poisson's ratio. Such materials, called functionally graded materials (FGMs), represent a class of materials in which compositions/constituents and/or microstructures gradually change along single or multiple spatial directions, resulting in a gradual change in properties and functions which can be tailored for enhanced performance.

FGMs can be obtained through two phases, for example metal and ceramic, whose volume fractions vary gradually, porous materials [1, 2] and additive manufacturing technologies [3, 4].

Optimization procedures are usually implemented in finite element codes. The dedicated software packages do not generally contain explicit implementation for modeling FGMs, as most of them use isotropic or anisotropic homogeneous materials. This drawback can be overcome by implementing finite elements with a nonhomogeneous material [5], but sufficiently good precision can be obtained by using refined meshes for which each element is considered an isotropic material [6, 7].

For simple FGM structures loaded symmetrically as spheres and thick-walled tubes or thin disks, were established stress conditions (circumferential or hoop stress and in-plane shear stress) for which the whole geometrical domain reaches constant values, i.e. *stress conditions for uniformization* (SCU). Necessary distributions of $E(r)$, if FGM is isotropic, were obtained in the hypothesis of keeping $\nu(r)$ = const. [8]. These kinds of problems in the optimization of thick-walled shells are based on solutions for inverse problems of the elastic theory of inhomogeneous bodies. Other stress conditions, such as classical theories of strength, used in solutions of inverse problems are presented in [9–12].

The effect of a non-constant Poisson's ratio upon the elastic field in functionally graded axisymmetric solids was analyzed for example in [13].

This paper is a continuation of our previous work starting with [14] and is mainly dedicated to the presenting of six significant case studies which demonstrate the possibility to design functionally graded spheres, cylinders and disks using a stress condition which is enforced to be constant along the body radius r. The stress condition may be one very simple, as linear combinations of principal stresses, an equivalent stress or even better, from practical point of view, a design or safety factor.

The paper is organized in six sections, as follows. In section two, the work briefly presents the analytical solutions (resented in detail previously) of optimum design solution for pressurized FGM spheres, cylinders and disks for the two most used stress conditions in literature: in-plane shear stress and circumferential stress to be constant. Section three presents some practical stress conditions in current design. In section four, the finite element models and the stress condition uniformization algorithm are briefly presented. Also, some homogenization relationships are summarized. In section five, for verification and pointing out the novelties of this paper, some practical case studies (applications) are given as examples. Comments on the results obtained are also presented. The paper ends with some general conclusions in the last section.

2. ANALYTICAL OPTIMAL SOLUTIONS

We consider a sphere/cylinder/disk with inner radius *a* and external radius *b*, loaded with interior pressure p_a and exterior pressure p_b, Fig. 1, and elastic inhomogeneous material (FGM) with radial symmetry.

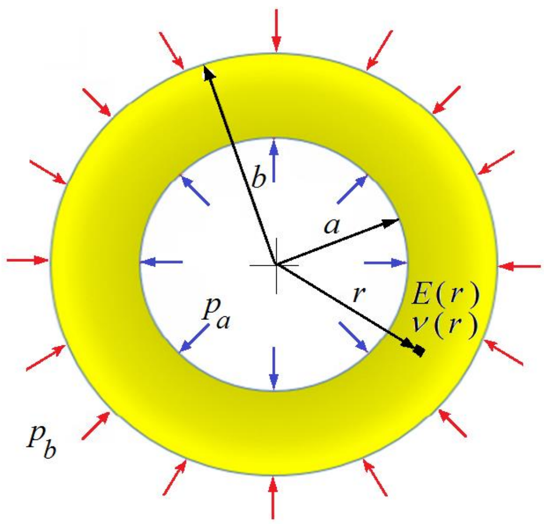

Fig. 1 – Isotropic inhomogeneous FGM sphere/cylinder/disk.

2. 1. STRESS CONDITION Opt 1

For stress condition Opt 1, i.e. $\sigma_r - \sigma_\theta = C_0$=const., results the expression which describes the variation of Young's modulus as a function of geometry, loading, and Poisson’s ratio (considered constant). It was obtained by the authors of this paper in [14]

$$E(r) = C_1 \left\{ p_a \left[1 + n_1 \log\left(\frac{r}{b}\right)\right] - p_b \left[1 + n_1 \log\left(\frac{r}{a}\right)\right]\right\}^{n_2} . \qquad (1)$$

In expression (1) C_1 is a constant of integration and the values of the parameters n_1 and n_2 are given in Table 1.

Table 1

Coefficients in Eq. (1) for particular axisymmetrical bodies if $\sigma_r - \sigma_\theta$ =const.

Coefficients	Sphere	Cylinder	Disk
n_1	$\frac{2(1-2\nu)}{1-\nu}$	$\frac{1-2\nu}{1-\nu}$	$1-\nu$
n_2	$\frac{3(1-\nu)}{2(1-2\nu)}$	$\frac{2(1-\nu)}{1-2\nu}$	$\frac{2}{1-\nu}$

2. 2. STRESS CONDITION Opt 2

For the condition Opt 2, i.e. $\sigma_\theta = D_0$ =const., it was obtained [14]

$$E(r) = C_2 \left\{ p_a \left(\frac{a}{b} \right)^{\chi} \left[1 + n_1 \left(\frac{b}{r} \right)^{\chi} \right] - p_b \left[1 + n_1 \left(\frac{a}{r} \right)^{\chi} \right] \right\}^{n_2}, \tag{2}$$

where C_2 is an integration constant, χ is the shape factor and n_1 and n_2 are different from the previous case and are given in Table 2.

Table 2

Coefficients in Eq. (2) for particular axisymmetrical bodies if σ_θ =const.

Coefficients	Sphere (χ = 2)	Cylinder (χ = 1)	Disk (χ = 1)
n_1	$\frac{\nu}{1-2\nu}$	$\frac{\nu}{1-2\nu}$	$\frac{\nu}{1-\nu}$
n_2	$\frac{\nu-1}{2\nu}$	$\frac{\nu-1}{\nu}$	$-\frac{1}{\nu}$

The distribution of the Young's modulus obtained in relations (1) and (2) must describe variations which fit in a relatively small interval because, practically, the variations obtained for a FGM material are of the order of units. This aspect is presented in detail in [14].

The use of a FGM instead of homogeneous material with $E(r)$ = const. is usually justified due to the reduction of the stress components in bodies made from such a material [14].

3. PRACTICAL STRESS CONDITIONS

Analytical solutions presented in Section 2, were established for particular conditions of distribution of stress, named Opt 1 and Opt 2. However, usually in practice is important the distribution of the equivalent stresses.

The normal stresses in an axisymmetrical body (radial, circumferential, axial) are sorted as principal stresses $\sigma_1 \geq \sigma_2 \geq \sigma_3$. If we assume that the allowable stresses in tension and compression are the same in absolute value, then the classical strength theories are [15]:

I. the maximum stress theory (Rankine);
II. the maximum strain theory (Saint Venant);
III. the maximum shear theory (Tresca);
V. the maximum distortion strain energy theory (von Mises).

The explicit relations of equivalent stresses are given in [16].

If the allowable stresses in tension and compression are different, in the literature sometimes the Mohr theory is used in the form

$$\sigma_{eqv}^{Mohr} = \sigma_1 - k\sigma_3, \tag{3}$$

where k is the ratio of the allowable stresses of the material in tension and compression.

For homogeneous materials, the uniaxial yield limit is a constant, but for inhomogeneous bodies discussed in this work, the yield limit is function of current radius, as $\sigma_y(r)$. Considering a particular strength theory, the structural safety or design factor is defined as

$$DF(r) = \frac{\sigma_{eqv}(r)}{\sigma_y(r)}. \tag{4}$$

In this paper the inverse of the design factor, i.e. the safety factor is defined as

$$c_i(r) = \frac{\sigma_y(r)}{\sigma_{eqv}^i(r)}, \tag{5}$$

where i = I, II, III or V marks the chosen strength theory. In design we are interested in the minimum value defined in (5), which normally must be larger than one. Both Eqs. (4) and (5) are stress conditions from a mathematical point of view. For an equal strength structure $c_i(r)$ = const.

4. FINITE ELEMENT MODELS AND SCU ALGORITHM

4. 1. THE USE OF FINITE ELEMENT MODELS

In most situations, to verify the results obtained analytically for the prescribed distribution of the material properties (the direct problem) many authors use the finite element method. This approach must establish how the spatially variable material properties can be described in the used software. Usually, the commercially available finite element software makes possible the assignment of a material with constant elastic properties to a certain finite element (homogeneous finite elements). This approach introduces errors. However, for meshes sufficiently refined the errors introduced by homogeneous finite elements are negligible. Because numerical errors are dependent on the finite element type, boundary conditions and gradient of material properties, a convergence study must be first developed to establish the final mesh size to be used in the analyses.

The conceptual models used in this paper are presented in Fig. 2. Due to the symmetrical conditions, for a sphere, only a sector of the model (Fig. 2a) is analyzed for an arbitrary angle θ. As to reduce the computational effort and increase the precision, at the limit an element can be considered in the circumferential direction and the θ angle very small, as to keep the aspect ratio close to one. The axisymmetric model for an infinite long cylinder (Fig. 2b) is a slice of constant thickness *h* for which the axial displacements (along OY) on the two faces are blocked. For efficiency only one finite element can be considered along the thickness. For a thin disk (Fig. 2c) the finite element model can be constructed for half of the thickness, also due to symmetry conditions.

It is to be underlined that the geometry from Fig. 2a can be used for modeling an infinite long cylinder (plane strain condition) or a very thin disk (plane stress condition). In this paper the two geometries are equivalent from numerical point of view with the models shown in Fig. 2b, respectively Fig. 2c.

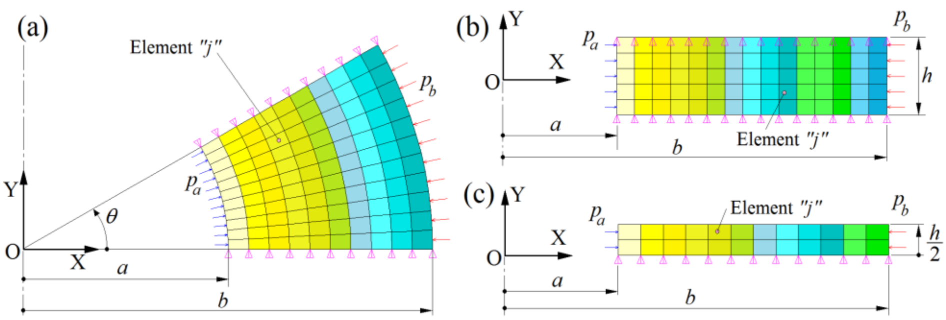

Fig. 2 – Axisymmetrical conceptual finite element models for sphere (a), cylinder (b) and disk (c). Every finite element j has a constant material property.

4. 2. ALGORITHM OF SCU

The theoretical stress condition can be any stress combination of stress tensor components including, if necessary, the uniaxial yield limit given as a function, for example $\sigma_y(r)$. In this section an arbitrary equivalent stress condition is used for the presentation of the developed algorithm. Uniformity is used to describe a desired constant stress condition. Normally in an axisymmetric FGM body a few functions such as $E(r)$, $\nu(r)$, $\rho(r)$ and $\sigma_y(r)$ are necessary to completely define the FGM. Normally these functions are not independent and, in literature, if the FGM is obtained using the homogenization theory, these functions are dependent on the volume fraction of the components. Usually, two constituents are used, and a single volume fraction $f(r)$ is sufficient to define all these functions $E(f(r))$, $\nu(f(r))$, $\rho(f(r))$ and $\sigma_y(f(r))$. Because the most important in the presented algorithm is the variation $E(r)$, we call it *driven function*. If we know $E(r)$, then, from $E(f)$ which normally is a monotonic function in the homogenization theories, we can obtain $f(E)$ and then $\nu(E)$, $\rho(E)$ and $\sigma_y(E)$. So, the secondary parameters $\nu(r)$, $\rho(r)$ and $\sigma_y(r)$ are functions of the driven function and the number of unknowns can be drastically reduced. In practice, for a particular problem, $\nu(E)$, $\rho(E)$ and $\sigma_y(E)$ may be explicitly given also as functions obtained using fitting methods.

For the finite element model, meshed with a total of n finite elements, the Young's moduli of all elements $E^j,\ j=1\ldots n$, are considered as a design variable vector

$$\boldsymbol{X} = \begin{bmatrix} E^1 & E^2 & \cdots & E^n \end{bmatrix}. \tag{6}$$

For each finite element, it is associated with an average value of the equivalent stress $\sigma_{eqv,j}$. A function $F: R^n \to R$ can be defined through the extreme global values of the equivalent stresses in the model, $\sigma_{eqv,\max} = \max_j\left(\sigma_{eqv,j}\right)$ and $\sigma_{eqv,\min} = \min_j\left(\sigma_{eqv,j}\right)$. Then the following function is defined

$$F\left(\boldsymbol{X}\right) = \sigma_{eqv,\max} - \sigma_{eqv,\min}\,. \tag{7}$$

If the extreme values of the equivalent stresses are equal, then $F\left(\boldsymbol{X}\right)=0$ and the equivalent stresses are constant and uniformly distributed over the whole domain. The problem of optimization *minmax* becomes a continuous variable optimization criterion

$$\textit{Minimize} \quad F\left(\boldsymbol{X}\right), \ \text{objective function} \tag{8}$$

which may be optionally subject to side constraints

$$E_{\min} \le E^{j} \le E_{\max}; \quad j = 1 \ldots n. \tag{9}$$

In practice $E_{\min}$ and $E_{\max}$ define the domain of acceptable values for the considered design variables.

Using the adapted fully stressed design algorithm [17, 18], or uniformization of the stress condition in this paper, the relation of iterative correction of the modulus of elasticity was chosed as

$$E_{(i)}^{j} = E_{(i-1)}^{j}\left[1 + \delta_{(i)}\left(1 - \frac{\sigma_{(i-1)}^{eqv,j}}{\sigma_{(i-1)}^{eqv,\max}}\right)\right], \tag{10}$$

where:

- $\delta_{(i)}$ is a coefficient which defines the degree of modification of the modulus of elasticity at the current iteration and which in this work was maintained constant $\delta = \delta_{(i)}$. It may be updated each iteration to reduce the number of total iterations until convergence is obtained;

- $\sigma_{(i-1)}^{eqv,j}$ is the stress condition, which is to become uniform, as here the equivalent stress in element j at the iteration $(i-1)$;

- $\sigma_{(i-1)}^{eqv,\max}$ is the maximum equivalent stress for all finite elements at iteration $(i-1)$.

Initially, for $i = 1$, it is considered that all the elements j are made from the same material with the modulus of elasticity $E_0^j = E_{\min}$, and for each new iteration $(i+1)$, in each element the modulus of elasticity (as a design variable) is updated.

For stopping the computation (as a convergence criterion) the infinity norm of relative variation of the modulus of elasticity was used for the last two iterations,

$$\max_{j}\left(\frac{\left|E_{(i)}^{j} - E_{(i-1)}^{j}\right|}{E_{(i)}^{j}}\right) \le \varepsilon_E, \tag{11}$$

where one can chose $\varepsilon_E = 10^{-3} - 10^{-6}$.

The second condition for stopping computation is based on the extreme stresses obtained at the current iteration, that is

$$\frac{\sigma_{(i)}^{eqv,\max} - \sigma_{(i)}^{eqv,\min}}{\sigma_{(i)}^{eqv,\max}} \le \varepsilon_\sigma, \tag{12}$$

where ε_σ can be chosen in between $10^{-3} - 10^{-6}$. This last criterion is efficient for problems of FSD (fully stressed design) type, whereas the first one is useful for problems where constraints (9) are active. According to this constraint condition, it was considered: if $E_{(i)}^{j} < E_{\min}$, then $E_{(i)}^{j} = E_{\min}$ and if $E_{(i)}^{j} > E_{\max}$, then $E_{(i)}^{j} = E_{\max}$. In this work the iterations stop only when one of them, Eq. (11) or Eq. (12) are first fulfilled.

The algorithm was implemented in ANSYS APDL for the model presented in Fig. 2 using Plane182 or Plane183 element type. More details about implementation and convergence are given by Sorohan and Constantinescu [16, 19] and in the presentation of the next section.

4.3. HOMOGENIZATION OF MATERIAL PROPERTIES

Let's consider a FGM made of two distinct isotropic materials, for example, a metal phase 1, and a ceramic phase 2. For the two materials Young's modulus E_i, Poisson's ratio ν_i, mass density ρ_i and the yield limit σ_{yi}, i = 1, 2 are known. If volume fraction for material 2 is $V_2 = f$, then volume fraction for material 1 is $V_1 = 1 - f$. Bulk modulus and shear modulus for isotropic constituents may be obtained using $K_i = E_i \big/ \left[3\left(1-2\nu_i\right)\right]$ and $G_i = E_i \big/ \left[2\left(1+\nu_i\right)\right]$.

4. 3. 1. Rule of mixtures

According to this most popular homogenization approach, the effective material properties are

$$E = E(f) = (1-f)E_1 + f\,E_2, \tag{13}$$

$$\nu = \nu(f) = (1-f)\nu_1 + f\nu_2, \tag{14}$$

$$\rho = \rho(f) = (1-f)\rho_1 + f\rho_2, \tag{15}$$

$$\sigma_y = \sigma_y(f) = (1-f)\sigma_{y1} + f\sigma_{y2}. \tag{16}$$

The first two equations are questionable and in current literature many other homogenization techniques are presented.

The mixture rule (15) is a good approximation for the effective mass density ρ, and was used through this paper.

Normally if the phase 2 is ceramic there is not a yield limit, σ_{y2} in (16) but it is a good approximation if

$$\sigma_{y2} = \sigma_{y1}\left(\frac{q+E_1}{q+E_2}\right)\frac{E_2}{E_1}, \tag{17}$$

where q is the stress to strain transfer ratio and may be constant for relatively small volume fraction f as is presented in [20]. In this paper, we considered this relation true also for a large volume fraction f. Relations (16) and (17) are known in the literature as Tamura-Tomota-Ozawa model [1, 2] or updated (modified) mixture rule composites [21].

4.3.2. Mori-Tanaka scheme

Effective elastic moduli of quasi-isotropic and quasi-homogeneous multiphase materials of arbitrary phase geometry should satisfy the Hashin-Shtrikman lower and upper limits [22]. In this case E and ν are obtained based on the lower limits of K and G. Using this scheme, first the bulk modulus and the shear modulus are estimated using

$$K = K(f) = K_1 + f\frac{K_2 - K_1}{1 + (1 - f)\dfrac{3(K_2 - K_1)}{3K_1 + 4G_1}}, \tag{18}$$

$$G = G(f) = G_1 + f\frac{G_2 - G_1}{1 + (1 - f)\dfrac{6(G_2 - G_1)(K_1 + 2G_1)}{5G_1(3K_1 + 4G_1)}}. \tag{19}$$

Then, Young's modulus and Poisson's ratio are calculated, using

$$E = \frac{9KG}{3K + G}, \quad \nu = \frac{3K - 2G}{2(3K + G)}. \tag{20}$$

In the uniformization algorithm presented in section 4.2, we obtain an improved value only for E and we need to correct also ν, ρ and σ_y. The simplest case in practice is to have given explicit functions $\nu(E)$, $\rho(E)$ and $\sigma_y(E)$. Another possibility is to extract volume fraction f from $E(f)$ if a homogenization scheme is used and then having established the volume fraction the problem is trivial. Next, we present, for the two considered homogenization schemes, how can be extracted the volume fraction f if E is known.

4.3.3. Extracting volume fraction and Poisson's ratio if the effective Young's modulus is given

For the rule of mixtures this problem is very simple because there is a linear relationship between Young's modulus and the volume fraction. So, considering f from (13) and replacing it in (14) we obtain

$$\nu(E) = \nu_1 + \frac{E - E_1}{E_2 - E_1}(\nu_2 - \nu_1). \tag{21}$$

Similar relationships are obtained also for the mass density and the yield limit of the FGM. For Mori-Tanaka scheme, first we introduce the notations

$$\begin{aligned} v_1 &= K_2 - K_1, \quad v_2 = \frac{3(K_2 - K_1)}{3K_1 + 4G_1}, \\ v_3 &= G_2 - G_1, \quad v_4 = \frac{6(G_2 - G_1)(K_1 + 2G_1)}{5G_1(3K_1 + 4G_1)}, \end{aligned} \tag{22}$$

and (18), (19) become

$$K = K_1 + f\,\frac{v_1}{1 + (1 - f)v_2}, \tag{18'}$$

$$G = G_1 + f\,\frac{v_3}{1 + (1 - f)v_4}. \tag{19'}$$

Replacing (18') and (19') into (20,a) we obtain the equation

$$\frac{a_1 f^2 + b_1 f + c_1}{a_2 f^2 + b_2 f + c_2} = 0, \tag{23}$$

where coefficients a_1, b_1, c_1 and a_2, b_2, c_2 are functions of K_1, K_2, G_1, G_2, which are knows and are not given explicitly here because of their relatively long form. It can be checked that for real values of material properties, the denominator cannot be zero and solving $a_1 f^2 + b_1 f + c_1 = 0$, only one solution is valid, i.e. $0 \le f \le 1$. Having the volume fraction f, and using the relation (18), (19) and then (20b), we obtain numerically $\nu(E)$ if the Mori-Tanaka scheme is used in homogenization.

5. CASE STUDIES AND DISCUSSIONS

5. 1. CASE STUDY 1

This application, for a sphere loaded only with internal pressure, was mainly chosen as a mesh convergence study and validation of the proposed numerical algorithm.

The convergence analysis for a finite element model depends both on the finite element type chosen in the analysis and on the mesh refinement, and on the model geometry and boundary conditions. For the conceptual model from Fig. 2a, was considered the isoparametric axisymmetric finite element Q4 and a reduced integration (Plane182 in ANSYS). We consider a particular sphere with a = 100 mm; b = $\sqrt{\exp(1)}\cdot a \approx 164.8721$ mm; p_a = 100 MPa and p_b = 0. We look for the distribution of $E(r)$, $\sigma_\theta(r)$, $\sigma_r(r)$, $u(r)$, if $\nu(r)$ = 0.28323675 = const., as to uniformize the equivalent von Mises stresses (with same conditions for the Tresca criterion and σ_θ - σ_r = const.). To obtain a unique solution we choose $E_{\min} = E_a$ = 10 GPa. With these input data the extreme normal stresses are zero and ± 100 MPa, and the ratio E_b / E_a = 10.

As from a mathematical point of view the problem is unidimensional (1D) and the choice of angle θ is not important, we use the axisymmetric model (Fig. 2a) with θ small enough to have only a single element along circumferential direction. The model was uniformly meshed with an increasing number of elements along radial direction and keeping element shapes close to squares by the adequate choice of θ angle.

In the uniformization algorithm for the convergence criterion we considered $\varepsilon_E = \varepsilon_\sigma = 10^{-3}$. With the parameter δ = 1.4, the convergence solution is obtained in 11 iterations.

This problem has an analytical solution. To study the mesh convergence, the number of finite elements along the radial direction progressively increased from 5 to 2000.

It is to be underlined that the distribution obtained for $E(r)$ cannot be correctly described by a power low function as it is used in most cases in literature, but the variation which takes the exponential form of approximation [23], as

$$E(r) = E_a \exp\left(\frac{1-(r/a)^\eta}{1-(b/a)^\eta} \log \frac{E_b}{E_a} \right), \tag{24}$$

is good enough for getting $E(r)$ if $\eta \approx -1.78$, Therefore, the solutions can be verified by using the direct calculus presented in [23] and implemented also in MATLAB by the authors.

Relevant solutions, obtained for different meshes, are presented in Fig. 3. It is noticed that for a minimum of 100 elements on radial direction, the numerically obtained distribution of $E(r)$ is very close to the analytical one (Fig. 3a), the error being less than 5% (real value is underestimated) and increases at the ends of the interval (Fig. 3b). The error in obtained radial displacements is less than 3%, also underestimated (Fig. 3c), and the error for the obtained circumferential stresses is maximum at the limits of the interval (Fig. 3d) and can be both over- and underestimated. The variation curves for meshes with a very small number of elements show supplementary variations: ascending or descending (oscillations and jumps) as for each finite element constant elastic properties are considered (the conceptual finite element model is a theoretically multilayer homogeneous heterostructure model). It is worth noticing that the stresses calculated in the interior nodes over the sphere thickness are correctly estimated even for coarse meshes (Fig. 3d).

As the finite element model uses constant values of the material properties for each finite element, it is obvious to consider that the correct value of the variables corresponds to the center of the element. As to obtain the values of the variables in nodes (the smoothing of the step variation) one can consider the average value for the adjacent elements. For the finite elements at the limits of the domain, at r = a and r = b, there is only one node which takes the value corresponding to the element to which it is connected. This edge effect, because of the lack of an appropriate method of extrapolation, introduces large relative errors in the interpretation of the results for coarse meshes as it is presented in Fig. 3 for the mesh with only 5 elements in the radial direction. With the mesh refinement this effect is attenuated but does not disappear completely.

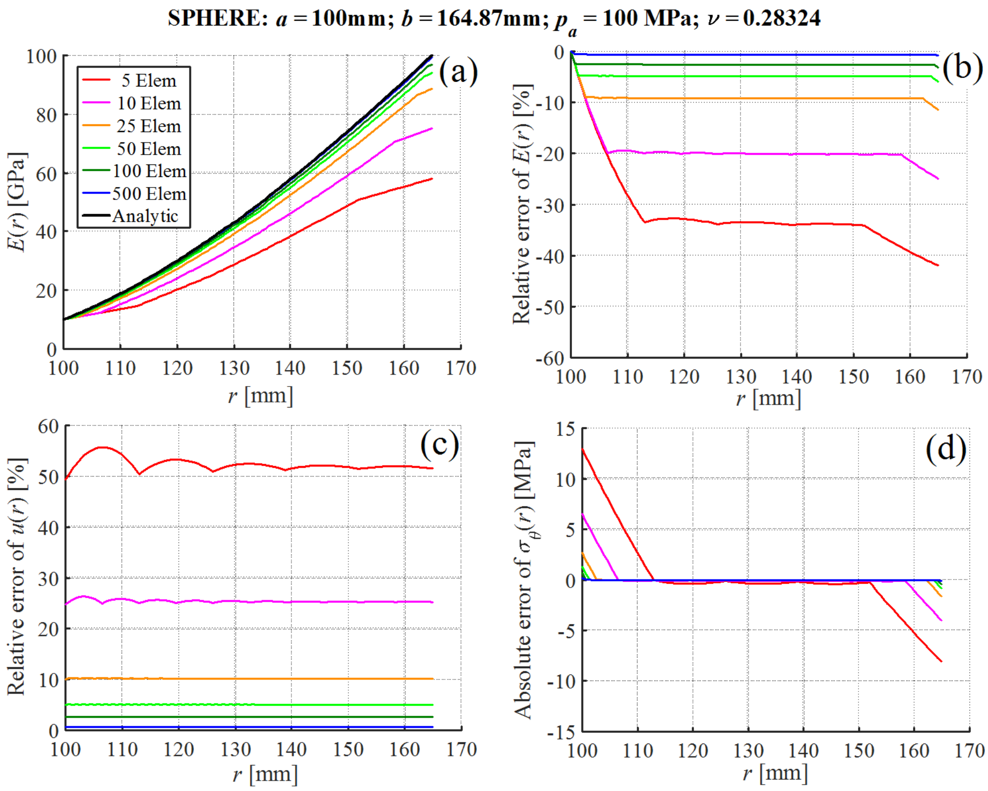

Fig. 3 – Solution and errors obtained in FEA for case study 1: a) Young's modulus distribution; b) relative errors of estimated Young's modulus; c) relative errors of radial displacement; d) absolute errors of circumferential stress.

The angle θ shown in the finite element model from Fig. 2 cannot be no matter small because the model of the sphere will tend to be the model of a cylinder. Through several trials it was established that the model for the sphere works correctly if $\theta \geq 0.125$ degrees. For this minimum angle and a non-uniform mesh with 5000 elements on radial direction and 10 elements in the circumferential direction, with a convergence error $\varepsilon_E = \varepsilon_\sigma = 10^{-3}$, the variation of $E(r)$ was between 10 GPa and 99.811 GPa, with a global estimation error of –0.19%. This cumulated error adds the edge effect discussed previously, as well as the convergence error, but also the inherent errors introduced by the finite element method. If the criteria for stopping the iterations was chosen to be $\varepsilon_E = \varepsilon_\sigma = 10^{-3}$, then theoretically one cannot obtain solutions with a precision greater than about 0.1% regardless of how refined the mesh is.

For a uniform mesh with 1000 elements in radial direction – knowing that the centroidal theoretical values of the moduli of elasticity in the inner finite element, respectively in the outer finite element are 10.0247 GPa and 99.941 GPa – after performing a FEA analysis the values are 10.0247 GPa, respectively 99.770 GPa. If we accept that the resulting values correspond to the edge nodes and not to the centroid of the end elements, then FEA gives: 10 GPa and 99.5246 GPa. Anyhow, for a uniform mesh with 1000 elements in a radial direction the errors are below 0.5%, although there are not done corrections as to compensate for the edge effects. The uniform mesh with 500 elements in radial direction ensures errors below 1% which are acceptable from practical point of view. For the following case studies, the meshes used for obtaining results are with a minimum of 500 elements in radial direction, but in most cases with 1000 elements. It was noticed that the mesh refinement does not influence the number of iterations as to reach the precision imposed by the stopping criterion. Keeping this in mind, and considering $\varepsilon_E = \varepsilon_\sigma = 10^{-3}$, is sufficient for reducing the number of iterations in the uniformization algorithm.

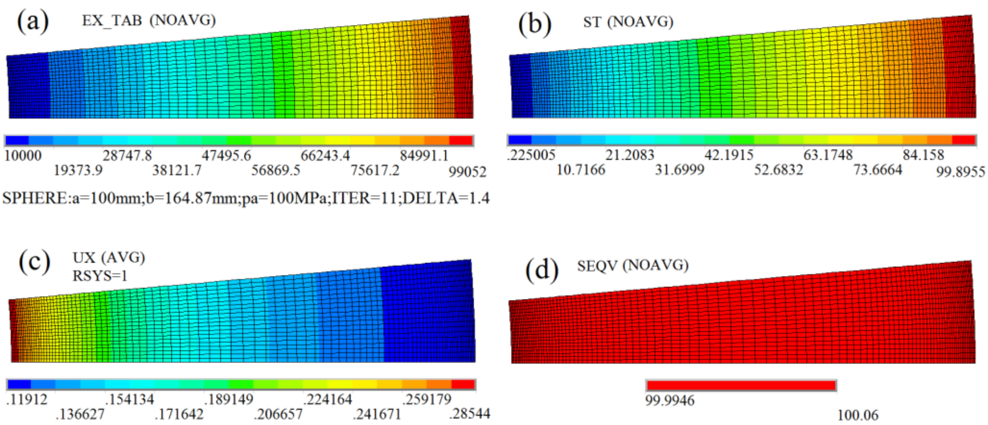

Fig. 4 – FEA solution for case study 1 when a non-uniform mesh is used: a) Young's modulus $E(r)$; b) circumferential stress $\sigma_\theta(r)$; c) radial displacement $u(r)$; d) equivalent stress $\sigma_{eqv}(r)$ which was imposed to be constant.

For a non-uniform mesh (element size smaller at the inner and outer surfaces of the sphere and larger in the middle part) with 100 elements in the radial direction and 20 elements in the circumferential direction (θ = 5 degrees), the results obtained by using FEA after 11 iterations, needed for attaining convergence, are presented in Fig. 4. Young’s modulus and stresses are in MPa and displacements in mm.

This figure shows that the algorithm works correctly even if the number of finite elements is increased in the circumferential direction (the problem is 1D from mathematical point of view), but also that the use of non-uniform meshing can lead to the reduction of the edge effects when keeping constant the number of finite elements in the mesh.

5. 2. CASE STUDY 2

This application, established for a set of spheres, all loaded only with external pressure, was chosen, in principle, for results validation compared to those from literature, as now we consider that Poisson’s ratio is variable, and therefore the analytical relations are not anymore valid.

As to separate the multiple obtained solutions, that is pairs of functions for $E(r)$ and $\nu(r)$, this application uses homogenization and the stress condition σ_θ = const., which corresponds here to the equivalent stress calculation by using the *I*st strength theory.

Nie *et al*. [8] consider a sphere (in fact three variants) with a = 10; 30 and 60 mm and b = 100 mm loaded only with external pressure: p_a = 0 MPa and p_b = 100 MPa and the distributions for $E(r)$ and $\nu(r)$ resulting by using the design condition of the FGM for σ_θ = const., that is Opt 2 with our notations. The volume fractions of two phases of FGM are assumed to vary only with the radius and the effective material properties are estimated by using either the rule of mixtures or the Mori–Tanaka (MT) scheme. The materials’ data for the constituents (metal and ceramic) are given in Table 3.

Table 3

Material properties for case studies 2–5

Material	Aluminum (material 1)	SiC (material 2)	Source
Young's modulus (GPa)	73	450	Nie *et al*. [8]
Poisson's ratio (–)	0.33	0.16	Nie *et al*. [8]
Mass density (kg/m^3)	2700	4400	Adopted from literature
Yield limit (MPa)	280	–	Adopted from literature
Stress to strain transfer ratio q (GPa)	90		Bhattacharyya *et al*. [20]

Figure 5 presents some significant results obtained with FEA and presented with lines and some results obtained by Nie et al. [8] shown by symbols with the similar colour, for the cases when they are available. As in this reference the results were presented only graphically, they were extracted point by point and transformed from non-dimensional values to dimensional ones. From Fig. 5a and Fig. 5b it is noticed that our values are almost identical to the reference ones. In the legend of these figures, it is notated with "Mix" and "MT" the schemes of homogenization mixtures and Mori–Tanaka. It is to be mentioned that in the chosen reference was considered the value $E_a = E_{\min}$ as corresponding to the homogenization done with a volume fraction for material 2 of 1%. The yield stress was estimated using Tamura-Tamota-Ozawa model [24].

In Fig. 5c – Fig. 5f are presented in the following order: variation of the volume fraction of ceramic (SiC) being below 55%, as maximum acceptable; equivalent stresses calculated for the Ist strength theory which resulted as being constant as it was imposed from the beginning; the yield stress (limit) of the homogenized material which increases together with $E(r)$, and respectively the safety factor, estimated as based on the same Ist theory, which has significant variations for each analyzed case.

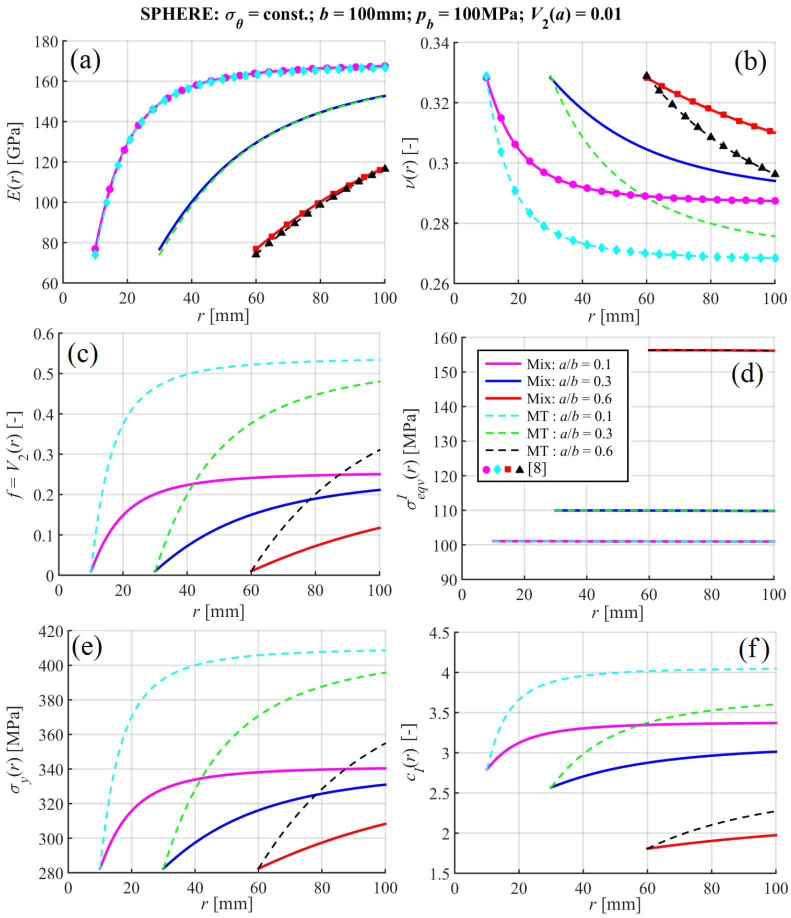

Fig. 5 – Results obtained for case study 2. Lines: FEA results; symbols: Nie *et al*. [8].

As the equivalent stresses according to the Ist strength theory are constant for all *r* values (Fig. 5d), these spheres are structures of equal loading but not of equal strength as the yield limit is not constant (Fig. 5e) and, as a result, the safety factors show relatively high variations (Fig. 5f). It is to be mentioned that uniform circumferential stress does not depend on the rule of homogenization.

5. 3. CASE STUDY 3

This application, for a cylinder loaded only with internal pressure, is also presented for results validation from literature. As in the previous application Poisson's ratio is variable and both stress conditions Opt 1 and Opt 2 in tailoring $E(r)$ and $\nu(r)$ are considered. This application also uses homogenization to separate the multiple solutions and the constituents' properties are the same as in the previous application (see Table 3).

In [8] is considered a cylinder with a = 60 mm and b = 100 mm (b / a = 1.6667) loaded with internal pressure p_a = 100 MPa and were obtained the distributions for $E(r)$ and $\nu(r)$ in the conditions $\sigma_\theta - \sigma_r$ = const. and σ_θ = const. along the radius. The volume fractions of two phases of FGM are assumed to vary only with the radius and the effective material properties are estimated by using either the rule of mixtures (Mix) or the Mori–Tanaka (MT) scheme. Here the yield stress was estimated using the Tamura-Tamota-Ozawa model.

The significant results obtained with FEA – shown with solid and dashed lines, and those from the mentioned reference (where available) shown with symbols, are presented in Fig. 6.

In [8] the results are given through functions obtained by fitting as using the least squares method. From Figs. 6a – Fig. 6c it is noticed that the results obtained with the algorithm proposed in this paper coincide with those from the mentioned reference. In [8] it was considered the value $E_a = E_{\min}$ for homogenization with a volume fraction of the material 2 equal to 0.00%.

In Figs. 6d – 6f are presented results in the following order: variation of radial displacements (Fig. 6d) which are maximum in the interior of the cylinder, larger if the average Young's modulus is smaller; the estimated safety factors based on the *I*st strength theory (Fig. 6e), which has minimum values both at the interior and at the exterior of the cylinder depending on the chosen stress condition; then the estimated safety factors based on the IIIrd strength theory (Fig. 6f), where the minimum values are to be obtained in the interior of the cylinder regardless the used stress condition and are smaller than those obtained by using the *I*st theory.

5. 4. CASE STUDY 4

This application is like the one presented for case study 2, but this time for a cylinder with a relatively large b / a, loaded only with external pressure and using stress condition Opt 2, as this option ensures a relatively small interval of variation for $E(r)$, that is E_b / E_a is relatively small.

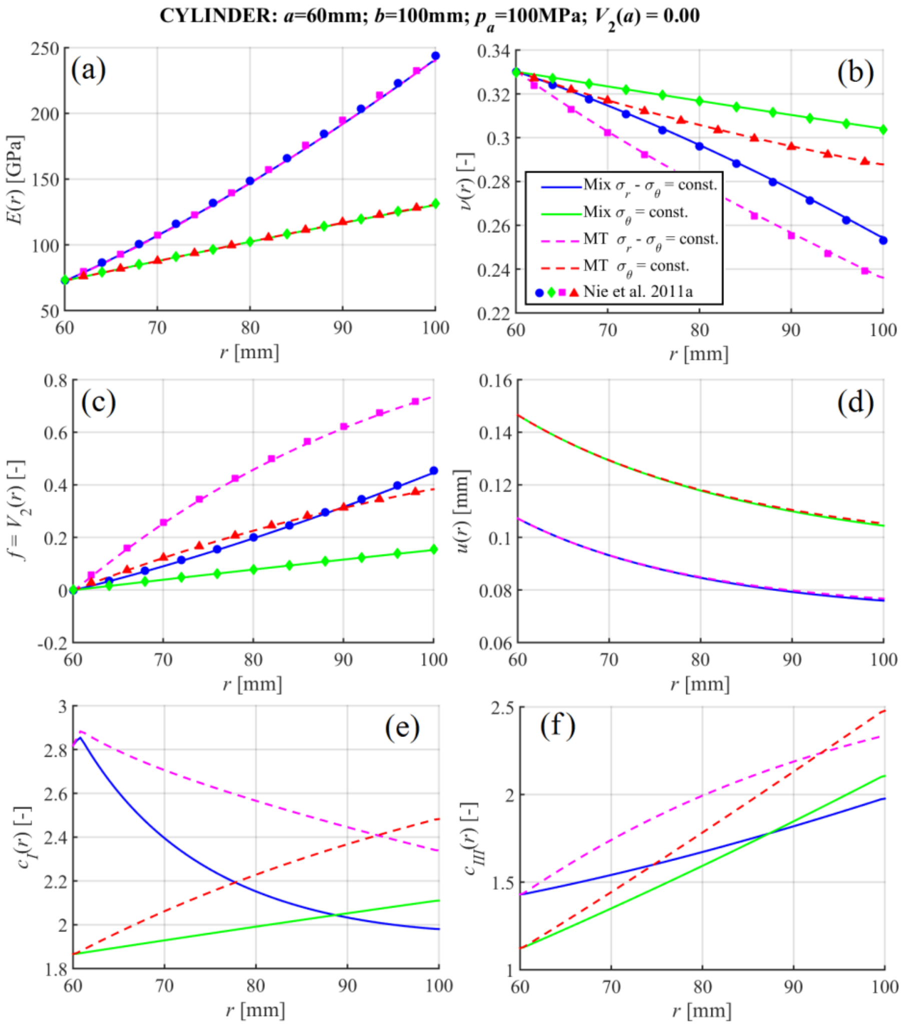

Fig. 6 – Results obtained for case study 3. Lines: FEA results; symbols: Nie *et al*. [8].

Initially the chosen geometry was the one used previously in literature, but afterwards the geometry was modified a little bit as to obtain an equal-strength structure imposing the design factor given in Eq. (4) which can be calculated with any of the equivalent stresses. Poisson's ratio is considered variable and for the separation of multiple solutions the method of homogenization is again considered.

The reference used previously for comparisons, [8], considers a cylinder with a = 10 mm and b = 100 mm loaded by external pressure p_b = 100 MPa, and are obtained the distributions of $E(r)$ and $\nu(r)$ when the hoop stress σ_θ = const. along the radius. The effective material properties are estimated by using either the rule of mixtures (Mix) or the Mori–Tanaka (MT) scheme. Input data are the same as for case study 2, as Table 3 is used. The volume fraction of SiC at the interior of the cylinder is imposed as 3%, that is $V_{2a} = 0.03$, which leads, by using relations (13) and (20a), to $E_a = E_{\min} = 84.3100$ GPa for the rule of homogenization mixture and $E_a = E_{\min} = 76.3577$ GPa for Mori–Tanaka. The yield stress was estimated using Tamura-Tamota-Ozawa model.

The results obtained with FEA are shown with continuous lines and the results taken from the mentioned reference (where they exist) represented by symbols are presented in Fig. 7. From Fig. 7a and Fig. 7b it is noticed that in fact the results obtained with the proposed algorithm in this paper coincide with those from the reference. In Fig. 7c is presented the variation of the volume fraction of SiC which has maximum values acceptable from theoretical point of view, bellow 80% for Mori–Tanaka and below 65% for the mixtures.

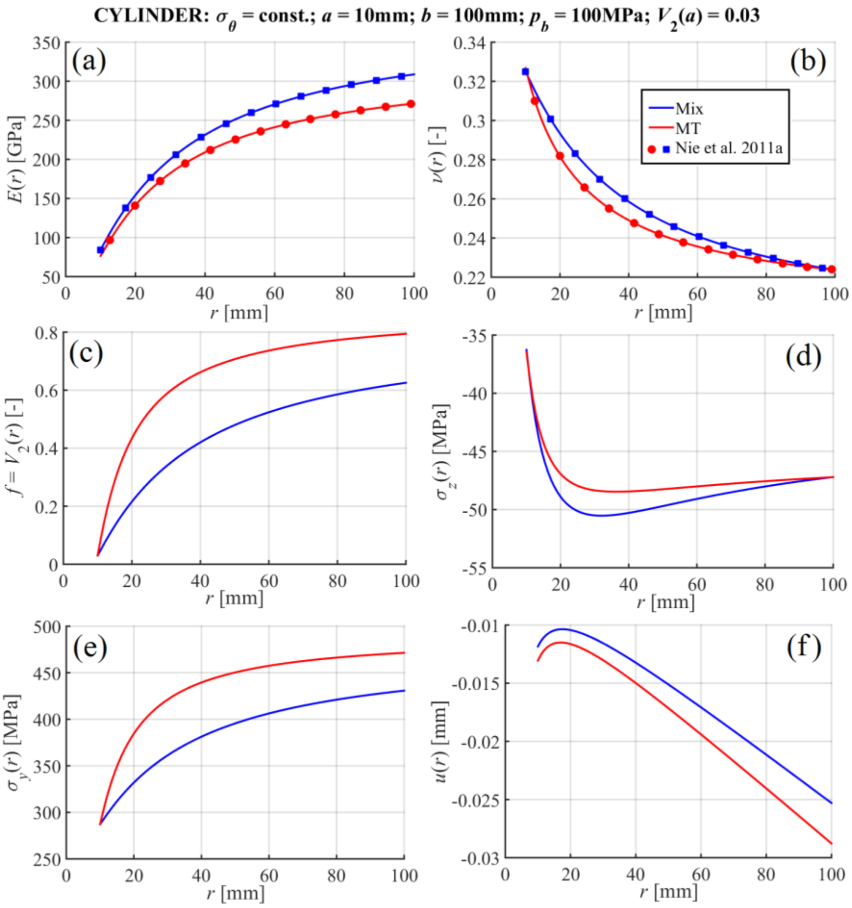

Fig. 7 – Results obtained for case study 4.

The distributions of the radial and circumferential stresses do not depend on the method of homogenization (σ_θ = const. = −111 MPa), but the axial ones do vary as shown in Fig. 7d. With the *I*st strength theory was obtained a structure of equal stress but not of equal strength because the yield limit of the homogenized material (Fig. 7e) is not constant and therefore the safety factor is not constant. As the modulus of elasticity depends on the homogenization method it results, consequently, that the radial displacements will have also a variation (Fig. 7f).

As the design may be done under the assumption of constant safety factors, the equivalent stresses were calculated by using the classical strength theories. For the initial geometry *b* / *a* = 10, the distributions for *E*(*r*) cannot fit into the available volume fraction domain for the homogenized material and therefore the interior radius *a* was increased as to obtain $V_2(r) < 1$ for all design criteria. For all the presented results the Mori-Tanaka scheme was used and $V_2(a) = 0.00$. Some of the significant results are shown on Fig. 8.

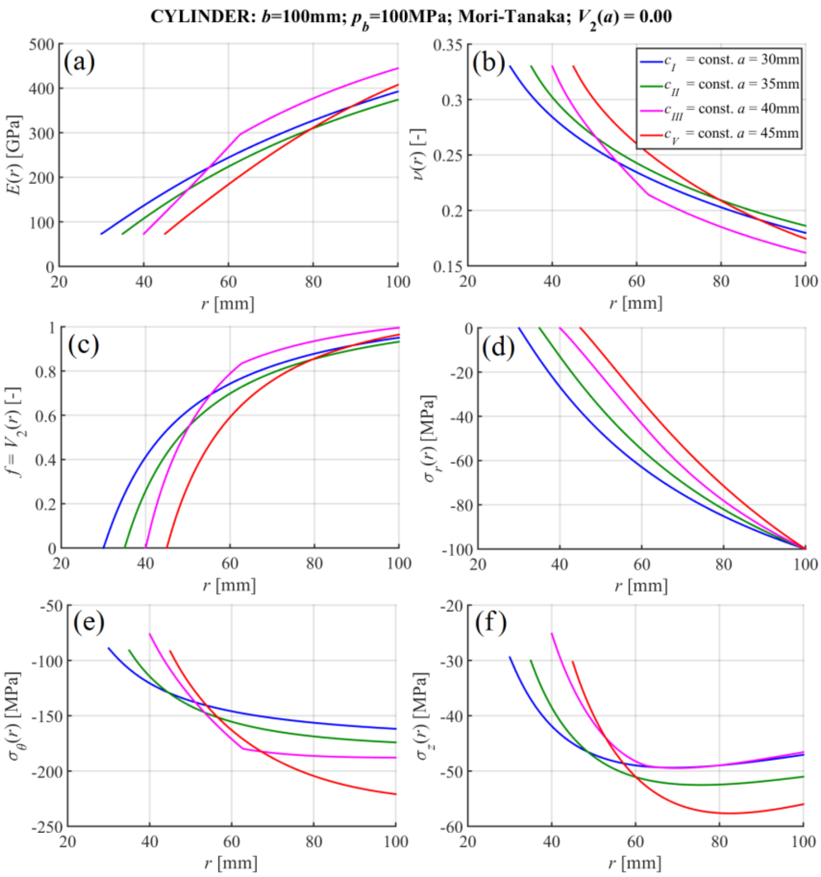

Fig. 8 – Results obtained for case study 4 using Mori-Tanaka homogenization and stress conditions for equal strength structures for four strength theories.

In the order of the strength theories with which were calculated the equivalent stresses, I, II, III and V, the thickness of the wall cylinder was reduced to a = 30; 35; 40 and 45 mm. From Figs. 8a to 8c it is noticed that the variation of the material properties $E(r)$, $\nu(r)$ and volume fraction $f(r) = V_2(r)$ is in between the properties of the two constituent materials and functions are continuous also in slope (C^1), except for the design done according to c_{III} = const. where we obtained piecewise functions (C^0). Figures 8d to 8f present the variations of the normal stresses. Fig. 8g shows the variation of the unidirectional yield limit. Figures 8h to 8k are giving the variations of the safety factors established as discussed, and Fig. 8l the one for the radial displacements.

Strength theory V ensures a minimum safety factor which has the highest global when all strength theories are considered, although the von Mises stress is in this case of highest value, but it is attained at the exterior of the cylinder where the yield limit has also the highest value.

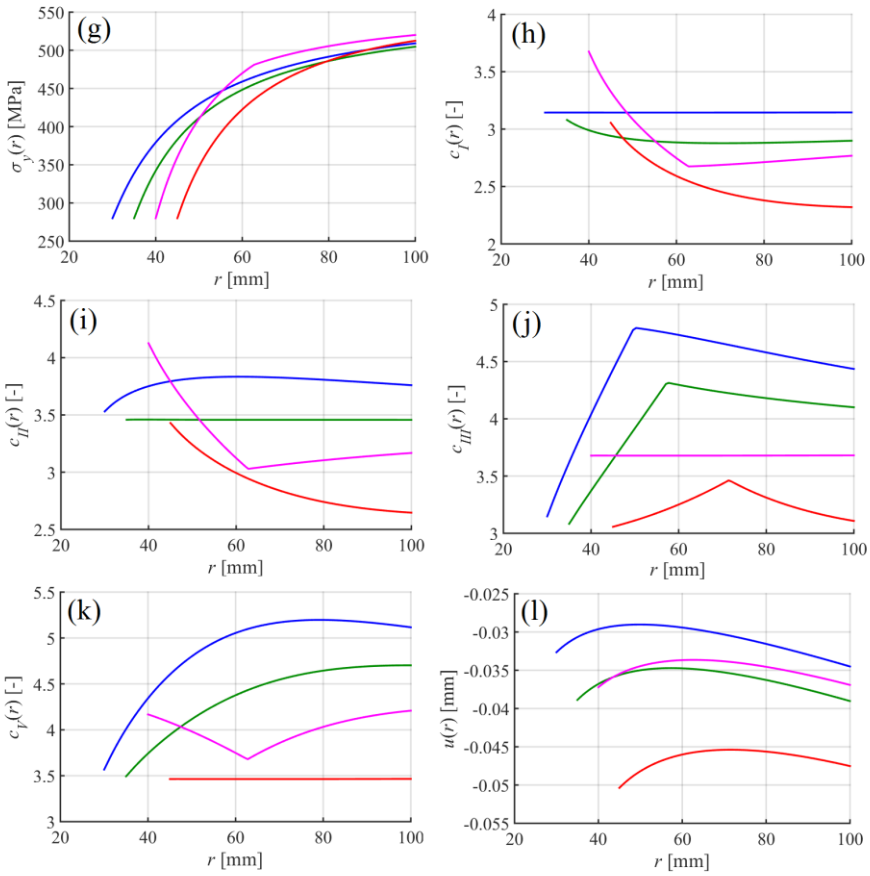

Fig. 8 – (Continuation). Results obtained for case study 4 using Mori-Tanaka homogenization and stress conditions for equal strength structures for four strength theories.

5. 5. CASE STUDY 5

In this example a FGM cylinder, loaded only with internal pressure, is designed according to different stress conditions uniformization, if the failure criteria for the FGM is according to von Mises equivalent stress. The target is to establish the maximum possible internal pressure in the condition of keeping the minimum safety factor to be one.

Case study 3 is reconsidered, but to obtain possible solutions in the conditions of uniformization of the safety factors, the ratio b / a is reduced to 1.5. We consider a cylinder with a = 100 mm and b = 150 mm. Material constants are the same, as defined in Table 3, and we accept for both the constituent materials and homogenized the failure criterion von Mises. Again, the imposed task is the following: to obtain the internal maximum pressure $p_{a,\max}$ which leads to a minimum safety factor equal to one when the Vth strength theory is used, that is $c_{\min}^{V} = 1$, regardless the stress condition for uniformization which is taken as already established: Opt 1 ($\sigma_\theta - \sigma_r$ = const.), Opt 2 (σ_θ = const.), and an additional one (theoretical) as coming from the Mohr theory $\sigma_\theta - k\sigma_r$ = const. (Eq. 3 with k = 2.73) and additionally by considering equal safety factors $c_i(r)$ = const., (i = I, II, III and V). The chosen geometry is kept the same and the maximum pressure is obtained.

As already mentioned, the criteria for uniformization can be considered as any established, being defined by stresses (stress components or their linear combinations), equivalent stresses, but also safety factors, strain density per unit volume, etc.

As the geometry is fixed, the relation between the stress conditions and the imposed internal pressure is linear, and in order to obtain $p_{a,\max}$ two analyses are needed: a preliminary one with p_a chosen randomly from which we get $c_{\min}^{V}$ and then $p_{a,\max}$ is established as to ensure $c_{\min}^{V}$ =1; then the analysis is redone as to obtain the final results.

For comparisons, two limiting cases are considered: one with Al as a homogeneous material, but also the theoretical one for SiC as a homogeneous material considering that its strength is higher.

Here the effective material properties are estimated by using the Mori–Tanaka scheme and the volume fraction of SiC for $r = a$, i.e. $f_a = V_{2,a} = V_2(r = a)$ = 0.00. The mass density was estimated by the rule of mixtures and the yield stress using Tamura-Tamota-Ozawa model.

The most important results obtained are shown in Fig. 9 and in Table 4. From Fig. 9, it is noticed that for all stress conditions checked in this application – there are seven considered, $E(r)$ varies within the limits theoretically admissible, the volume fraction for SiC does not exceed the value 1, and the variations of all variables are C^1 continuous and in agreement to the criteria imposed for uniformization. From Fig. 9h it is clearly observed that all safety factors calculated with the von Mises criterion ($\text{V}^{\text{–th}}$ theory) are greater than one, and the uniformization of the safety factor as $c_V(r)$ = const. = 1 is obtained. Values relatively close to one are obtained with the uniformization $c_{\text{III}}(r)$ = const., but also for $\sigma_\theta - 2.73\sigma_r$ = const. From Fig. 9i it is observed that the distributions of the radial displacements for FGM cylinders are in between the ones of the base homogeneous constituent cylinders.

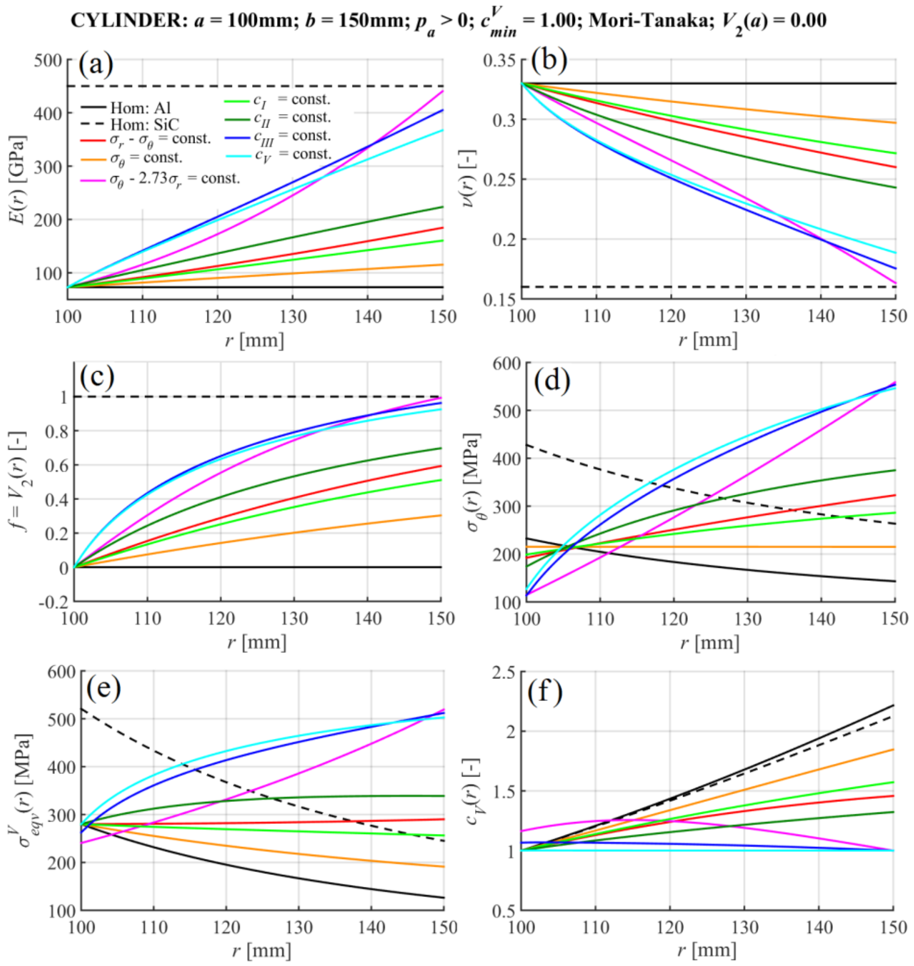

Fig. 9 – Results obtained for case study 5.

From the variation of the radial stresses (Fig. 9d) it is noticed a relatively large interval for the internal maximum pressure $p_{a,\max}$ obtained with SCU, the smallest pressure corresponding to the Al homogeneous material and the highest for the FGM obtained from the condition of uniformization of the safety factor calculated by using *V*th strength theory.

As it is known, for a homogeneous cylinder, the maximum circumferential stresses are obtained on the interior surface (Fig. 9e) and are decreasing towards the exterior, but for all analyzed variants of FGMs the variation is inversed, that is maximum value is at the exterior with a maximum gradient of uniformization of c_{III}, c_V, and $\sigma_\theta - 2.73\sigma_r$ which lead to the highest gradient in the distribution of $E(r)$, as it can be checked in Fig. 9a.

For a homogeneous cylinder the axial stress is constant, but for a FGM axial stresses are variable and are obtained from the relation $\sigma_z = \nu\cdot(\sigma_r + \sigma_\theta)$.

From Table 4 some conclusions can be drawn, among which: for the chosen dimensions of the cylinder (b / a = const.), and the consideration of the von Mises criterion, the FGM internally pressurized cylinder which allows the highest internal pressure and in the same time has the smallest specific mass as m / $p_{a,\max}$ = 0.7684 is the one designed in the condition of uniformization of the safety factor by using the *V*th strength theory. However, for this case, the ratio E_b / E_a = 5.03, that is the gradient of variation for $E(r)$ is a relatively high one, which constitutes a severe limit in the FGM cylinder practical realization. As compared to the homogeneous Al cylinder for which the specific mass is m / $p_{a,\max}$ = 1.1851, the designed FGM cylinder gives a relative decrease of this important design parameter with 35.16 % which confirms the benefits of using a FGM structure. Comparing the maximum internal pressure obtained for the FGM cylinder to the Al one, it can be increased with 119% that is more than double.

Table 4

Details of the designed cylinders for case study 5

No.	Stress condition for FGM uniformization	$p_{a,\max}$ (MPa)	E_b/E_a (-)	Mass m (kg/m)	m / $p_{a,\max}$ (kg/m/MPa)
1	NA (Aluminum)	89.47	1.000	106.03	1.1851
2	NA (SiC)	164.62	1.000	172.79	1.0496
3	$\sigma_\theta - \sigma_r$ = const.	130.94	2.526	129.49	0.9889
4	σ_θ = const.	107.55	1.578	117.77	1.0950
5	$\sigma_\theta - 2.73\sigma_r$ = const.	162.90	6.033	148.33	0.9106
6	c_I = const.	124.07	2.196	126.36	1.0185
7	c_{II} = const.	149.38	3.060	136.61	0.9145
8	c_{III} = const.	189.40	5.547	151.91	0.8021
9	c_V = const.	195.84	5.031	150.49	0.7684

5. 6. CASE STUDY 6

Abdalla et al. [25] considered an FGM sphere/cylinder/disk with a = 20 mm and b = 40 mm (b / a = 2) loaded with internal pressure p_a = 10 MPa and they obtained the distribution of $E(r)$ and $\nu(r)$ in the condition of minimizing the Tresca stress (σ_θ – σ_r = const.) only on a limited portion of the interior part of the axisymmetrical structure. In the mentioned paper FGM is obtained using different homogenizations techniques. Because in this case the effect of adopted homogenization technique is not very important for obtaining global results, in the present paper the Mori–Tanaka scheme for getting Young's modulus and Poisson's ratio was adopted. For mass density the rule of mixtures scheme was used and for the yield limit, the Tamura-Tomota-Ozawa model. The constituent materials and their properties given in the mentioned paper or taken from literature and used in simulation are presented in Table 5.

Table 5

Material properties used in case study 6

Material	Steel Material 1	Alumina (Al_2O_3) Material 2	Source
Young's modulus [GPa]	210	390	Abdalla et al. [25]
Poisson's ratio [-]	0.33	0.25	Abdalla et al. [25]
Mass density [kg/m^3]	7800	3900	Abdalla et al. [25]
Yield limit [MPa]	360	-	Adopted from literature
Stress to strain transfer ratio q [GPa]	90		Bhattacharyya et al. [20]

For these input data, where E_b / E_a is small, solutions cannot be obtained for $\sigma_\theta - \sigma_r$ = const. with $a \le r \le b$ because $E(r)$ established theoretically does not fit in the interval allowed by the two materials [14]. In our case, $E(r)$ which can be practically attained is within a narrow interval of variation as $(E_b / E_a)_{\max} = 390/210 = 1.857$. However, the maximum stresses in the analyzed structures can be reduced if a FGM is properly established in their interior. These aspects were discussed in several references [26 – 28].

The algorithm of stresses uniformization proposed in this paper leads to optimized solutions similar to those obtained by Abdalla et al. [25] as it activates the restrictions established in Eq. (9) of limiting the variations of $E(r)$. In order to discuss the effect of the geometry (sphere/cylinder/disk) upon the results, the present application presents in parallel the results obtained for the three bodies considered as being homogeneous and made from steel. Therefore, in Fig. 10 are presented the most important results obtained with the algorithm discussed in Section 4.2.

It is to be noticed that the results for cylinder and disk are very close, except the axial stresses which are zero for the disk (Fig. 10e). The equivalent stresses remain constant in the interior part of the body (Fig. 10g), and the safety factors increase (Fig. 10h) as the yield limit of the homogenized material increases also. If we compare the sphere with the cylinder/disk it is noticed that the transition from a “soft” material to a “rigid” material (Fig. 10a) is done for a double value of the radius for the cylinder and the disk compared to the sphere for which the FGM radius is about 3 mm. The radial displacements (Fig. 10i) for the sphere are smaller than for the cylinder.

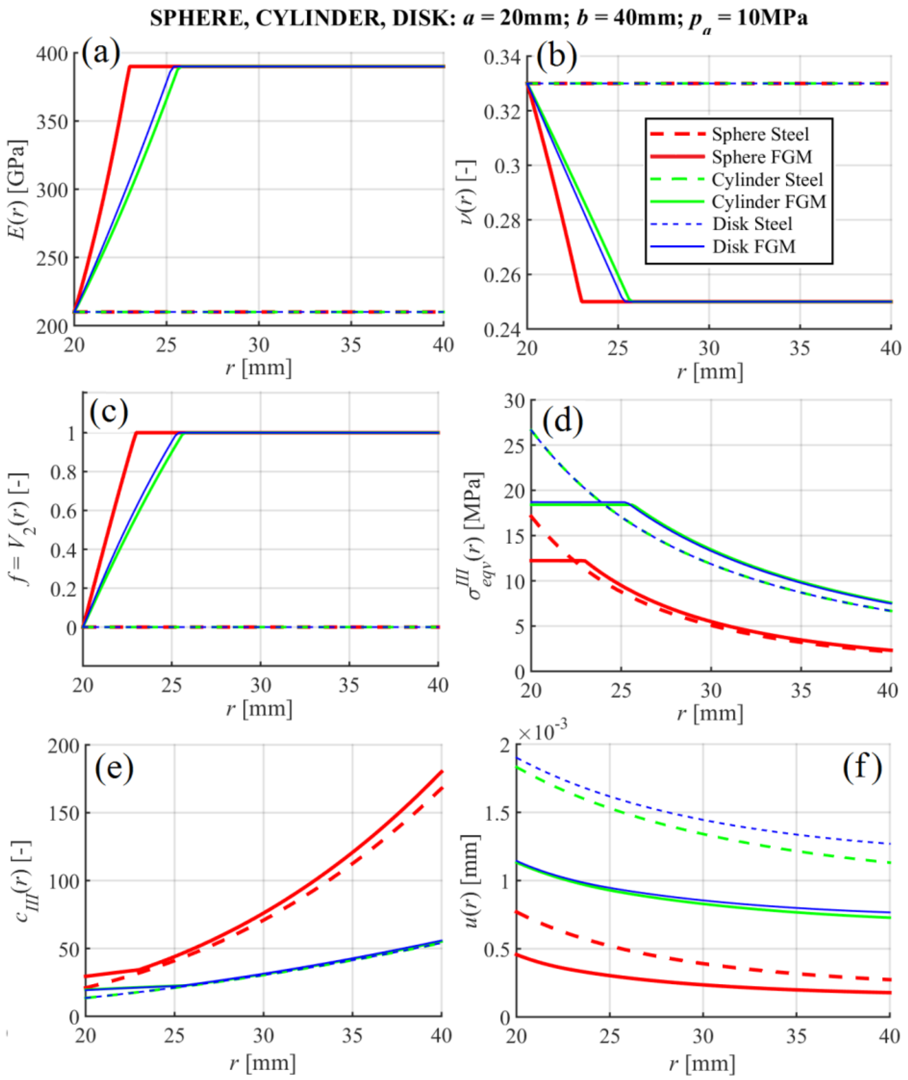

Fig. 10 – Numerical results using FEA obtained for the case study 6, using the uniformization of the Tresca stress.

For the input data considered in the case study it results that introducing a FGM in a relatively reduced zone in the interior of the bodies, which are softer where pressure is applied, the local state of stress can be reduced considerably, leading to the increase of the safety factors and, more significantly, to the important reduction of the mass of the structures. Evidently that these conclusions are valid in the context of these application, and we can notice that: *i*) the mass of the nonhomogeneous sphere is reduced with 48.27 %, the minimum value of the safety factor increases with 39.96%, and the maximum equivalent stress is reduced with 28.55%; *ii*) the mass of the nonhomogeneous cylinder is reduced with 45.10 %, the minimum safety factor increases with 44.73%, and the maximum equivalent stress is reduced with 30.91%; *iii*) the mass of the nonhomogeneous disk reduces with 45.53 %, minimum safety factor increases with 42.50%, and the maximum equivalent stress reduces with 29.83%.

The safety factors can be slightly increased if instead of using a criterion for the uniformization of equivalent stresses is used a criterion for the uniformization of the safety factors. As an example, if the sphere is uniformized the factor c_{III}, then the safety factor obtained previously as 29.4 becomes 30.2, and the transition zone from steel to alumina is reduced from about 3 mm to 2 mm.

6. GENERAL CONCLUSIONS

The principal contribution of this paper is the numerical approach for solving problems for which the analytical solution is difficult to obtain or does not exist. From numerical point of view, the main outcomes of this paper can be synthetically described by:

1. Presentation of finite element models adapted for the proposed problem, which can be used for both the direct problem but also for the inverse problem. For the inverse problem it was developed a simple, efficient and robust algorithm for uniformizing the stresses, named SCU, which iteratively corrects the distribution of $E(r)$, but also of $\nu(r)$, respectively of other important variables as the density $\rho(r)$, and the yield limit of a FGM, $\sigma_y(r)$, if the relations in between them are considered by using the theory of homogenization.
2. Solutions for the design of FGM bodies were obtained in the conditions of equal stress and equal strength (by using pertinent data for materials from literature) pointing out that the design of FGM structures can lead to the increase of possible loading capacity, but also to the decrease of the total mass of the body.
3. The algorithm of uniformization proved to be efficient also for solving situations in which there are restrictions imposed on the interval of variation of Young's modulus, as it is presented for case study 6. Also, more complex bodies geometries can be solved.

As the properties of FGMs have a relatively high degree of randomness, although the design (tailoring) method proposed in this paper can introduce errors of about 1% as the used meshes cannot be extremely refined and an iterative algorithm is used, the obtained results are from a practical point of view sufficiently precise. The SCU algorithm proposed in this work and implemented in Ansys APDL is robust and efficient. If the solution exists and is unique the algorithm converges towards it in a reasonable number of iterations, in between 5 and 25, function of the desired precision and the setting of the parameter $\delta_{(i)}$ from relation (10). The unicity of the solution is governed by the properties of the material chosen at the interior and exterior of the analyzed body. If the relation of constraints (9) is activated, then the uniformization for the stress condition may be incomplete as it is presented for case study 6. The presented SCU algorithm was validated by the authors for many chosen examples, but also on those identified in the literature as those presented by Andreev [9, 10], and Chepurnenko et al. [18].

To the best knowledge of the authors, the only solution of equal strength structure when $\sigma_y(r)$ is not constant was presented by Andreev [9], but for another strength condition. The solution was obtained using a semi-analytical technique, as initially the necessary equation was obtained analytically but its solution was obtained using the Runge-Kutta fourth order method.

As future directions for developing this research we aim to include the thermal effects, the optimization of the coefficient $\delta_{(i)}$ which gives the degree of modification of the modulus of elasticity at current iteration (as to reduce the number of iterations till the convergence of the algorithm), including the orthotropic functionally graded materials and a study of the problems for which are imposed restrictions on the variation of the Young's modulus which may be more useful in practice.

Acknowledgements. This work was supported by a grant from the National Program for Research of the National Association of Technical Universities – GNAC ARUT 2023, contract no.11/06.10.2023, code 112.

Received on June 9, 2025

REFERENCES

1. NIKBAKHT, S, KAMARIAN, S, SHAKERI, M., *A review on optimization of composite structures part II: Functionally graded materials*, Compos. Struct., **214**, pp. 83–102, 2019, https://doi.org/10.1016/j.compstruct.2019.01.105.
2. NAYAK, P., ARMANI A., *Optimal design of functionally graded parts*, Metals, **12**, 1335, 2022, https://doi.org/10.3390/met12081335.
3. ZHANG, C., CHEN, F., HUANG, Z., JIA, M., CHEN, G., YE, Y., LIN, Y., LIU, W., CHEN, B., SHEN, Q., ZHANG, L., LAVERNIA, E.J., *Additive manufacturing of functionally graded materials: A review*, Mater. Sci. Eng. A, **764**, 138209, 2019, https://doi.org/10.1016/j.msea.2019.138209.
4. EL-GALY, I.M., SALEH, B.I., AHMED, M.H., *Functionally graded materials classifications and development trends from industrial point of view*, SN Appl. Sci., **1**, 1378, 2019, https://doi.org/10.1007/s42452-019-1413-4.
5. SONDHI, L., THAWAIT, A.K., SANYAL, S., BHOWMICK, S., *Stress and deformation analysis of functionally graded varying thickness profile orthotropic rotating disk*, Mater. Today Proc., **33**, pp. 5455–5460, 2020, https://doi.org/10.1016/j.matpr.2020.03.258.
6. KIM, J-H., PAULINO, G.H., *Isoparametric graded finite elements for nonhomogeneous isotropic and orthotropic materials*, Trans. ASME, **69**, *4*, pp. 502–514, 2002, https://doi.org/10.1115/1.1467094.

7. NĂSTĂSESCU, V., MARZAVAN, S., *Functionally graded thick-walled tubes analysis by numerical methods*, Heliyon, **10**, e27309, 2024, https://doi.org/10.1016/ j.heliyon.2024.
8. NIE, G.J., ZHONG, Z., BATRA, R.C., *Material tailoring for functionally graded hollow cylinders and spheres*, Compos. Sci. Technol., **71**, *5*, pp. 666–673, 2011, https://doi.org/10.1016/j.compscitech. 2011.01.009.
9. ANDREEV, V.I., *Optimization of thick-walled shells based on solutions of inverse problems of the elastic theory for inhomogeneous bodies*, In *Computer Aided Optimum Design in Engineering*, **XII**, Eds. Hernández, S., Brebbia, C.A., Wilde, W.P., pp. 189–202, WIT Press, 2012, https://doi.org/10.2495/OP120171.
10. ANDREEV, V.I., *Inverse problems of the inhomogeneous theory of elasticity for thick-walled shells*, Int. J. Comput. Methods Exp. Meas., **2**, *2*, pp. 202–216, 2014.
11. ANDREEV, V.I., CHEPURNENKO, A.S., JAZYEV, B.M., *Model of equal-stressed cylinder based on the Mohr failure criterion*, Adv. Mater. Res., **887**, pp. 869–872, 2014, https://doi.org/10.4028/www.scientific.net/AMR.887-888.869.
12 ANDREEV, V.I., POTEKHIN, I.A., *Equal strength and equal stress structures. Models and reality*, Adv. Eng. Res., **102**, pp. 232–236, 2017, https://doi.org/10.2991/icmmse-17.2017.36.
13. MOHAMMADI, M., DRYDEN, J. R., *Influence of the spatial variation of Poisson's ratio upon the elastic field in nonhomogeneous axisymmetric bodies*, Int. J. Solids Struct., **46**, *3-4*, pp. 788–795, 2009, https://doi.org/10.1016/j.ijsolstr.2008.09.030.
14. SOROHAN ST., CONSTANTINESCU D.M., APOSTOL D.A., *On the tailoring of radially FGM hollow spheres, cylinders and disks*, Ro. J. Techn. Sci. Appl. Mech., **69**, *2-3*, pp. 167−190, 2024.
15. TIMOSHENKO, S.P., GOODIER, J.N., *Theory of elasticity*, MC Graw-Hill, New York, 1951.
16. SOROHAN ST., CONSTANTINESCU D.M., *Tailoring of functionally graded spheres using a uniform stress condition*, Ro. J. Techn. Sci. Appl. Mech., **68**, *1*, pp. 81−96, 2023.
17. BAUMGARTNER, A., HARZHEIM, L., MATTHECK, C., *SK0 (soft kill option): the biological way to find an optimum structure topology*, Int. J. Fatigue, **14**, *6*, pp. 387−393, 1992, https://doi.org/10.1016/0142-1123(92)90226-3.
18. CHEPURNENKO, A., LITVINOV, S., MESKHI, B., BESKOPYLNY, A., *Optimization of thick-walled viscoelastic hollow polymer cylinders by artificial heterogeneity creation: Theoretical Aspects*, Polymers, **13**, *15*, 2408, 2021, https://doi.org/10.3390/polym13152408.
19. SOROHAN ST., CONSTANTINESCU D.M., *Stress Uniformization using Functionally Graded Materials*, Ro. J. Techn. Sci. Appl. Mech., **66**, *2*, pp 167−181, 2021.
20. BHATTACHARYYA, M., KAPURIA, S., KUMAR, A.N., *On the stress to strain transfer ratio and elastic deflection behavior for Al/SiC functionally graded material*, Mech. Adv. Mater. Struct., **14**, pp. 295−302, 2007, https://doi.org/10.1080/15376490600817917.
21. SABER, E., ABD_ELSALAM, A., *A theoretical model for investigating the thermo-mechanical performance of functionally graded rotating discs with varying grading index values*, Forces Mech., **8**, 100103, 2022, https://doi.org/10.1016/j.finmec.2022.100103.
22. HASHIN, Z., SHTRIKMAN, S., *A variational approach to the elastic behavior of multiphase minerals*, J. Mech. Phys. Solids, **11**, *2*, pp. 127−140, 1963, https://doi.org/10.1016/0022-5096(63)90060-7.
23. ZAMANI NEJAD, M., ABEDI, M., LOTFIAN, M.H., GHANNAD, M., *An exact solution for stresses and displacements of pressurized FGM thick-walled spherical shells with exponential-varying properties*, J. Mech. Sci. Technol., **26**, pp. 4081–4087, 2012, https://doi.org/10.1007/s12206-012-0908-3.
24. TAMURA, I., TOMOTA, Y., OZAWA, M., *Strength and ductility of iron-nickel-carbon alloys composed of austenite and martensite with various strength*, Proceedings of the 3rd International Conference on Strength of Metals and Alloys, Cambridge, 20–25 August 1973, pp. 611–615.

25. ABDALLA, H.M.A., BOUSSAA, D., SBURLATI, R., CASAGRANDE, D., *On the best volume fraction distributions for functionally graded cylinders, spheres and disks - A pseudo-spectral approach*, Compos. Struct., **311**, 116784, 2023, https://doi.org/10.1016/j.compstruct.2023.116784.
26. YOU, L.H., ZHANG, J.J., YOU, X.Y., *Elastic analysis of internally pressurized thick-walled spherical pressure vessels of functionally graded materials*, Int. J. Press. Vessels Pip., **82**, *5*, pp. 347–354, 2005, https://doi.org/10.1016/j.ijpvp.2004.11.001.
27. ZHENG, C., LI, X., MI, C., *Reducing stress concentrations in unidirectionally tensioned thick-walled spheres through embedding a functionally graded reinforcement*, Int. J. Mech. Sci., **152**, pp. 257–267, 2019, https://doi.org/10.1016/j.ijmecsci.2018.12.055.
28. ZHENG, C., ZHANG, G., MI, C., *On the reduction of stress concentrations in thick-walled hollow spheres under an arbitrary uniform axial symmetric outer traction*, Int. J. Press. Vessels Pip., **194**, *Part B*, 104545, 2021, https://doi.org/10.1016/j.ijpvp.2021.104545.